Scaling of Fracture Response in Over-height Compact Tension Tests

Xiaodong Xu[a]*, Michael R. Wisnom[a], Yusuf Mahadik [a], Stephen R. Hallett[a]

[a]Advanced Composites Centre for Innovation & Science (ACCIS), University of Bristol, University Walk, Bristol BS8 1TR, UK

ABSTRACT

An experimental investigation into in-plane scaled Over-height Compact Tension (OCT) $[45/90/\text{-}45/0]_{4s}$ carbon/epoxy laminates was carried out to study the scaling of fracture response. The dimensions of the baseline specimens were scaled up and down by a factor of 2. Interrupted tests were carried out for specimens of each size in which the tests were stopped after certain load drops in order to study the failure mechanisms. X-ray Computed Tomography (CT) scanning was applied after the interrupted tests to examine the damage development and its effect on the fracture response. The test results showed that the scaling of the initial propagation of fracture follows Linear Elastic Fracture Mechanics (LEFM), but the development of the damage process zone differs with specimen sizes. The OCT specimens were found to be not large enough to generate a self-similar damage zone during propagation, and so no conclusions could be drawn regarding the R-curve effect.

Keywords: A. Laminates; B. Fracture toughness; D. Mechanical testing; Scaling

* Corresponding author. Tel.: +44 (0)117 33 15504; fax: +44 (0)117 954 5666
E-mail address: xiaodong.xu@bristol.ac.uk (X. Xu)

1. Introduction

Fracture toughness is an important parameter for composite structures. Though test standards are available for the measurement of plane strain fracture toughness for metallic materials [1] and trans-laminar fracture toughness for composite materials [2], the fracture response of composite laminates is still not well understood in terms of damage development and scaling. The Over-height Compact Tension (OCT) test was developed to determine fracture properties of composite laminates. The OCT specimen is regarded as being compact, exhibiting stable damage growth and allowing a post-test investigation of the damage evolution [3]. Damage development in OCT tests was investigated by Floyd [4], Williams et al. [5] and Li et al. [6]. Previously, a series of centre-notched tensile tests has shown that the scaling of in-plane dimensions of notched quasi-isotropic composite laminates shows a corresponding scaling of the damage zone with the size approaching a constant at large notch lengths [7]. The fracture toughness approaches an asymptote, as expected, based on LEFM. However, with such a specimen configuration, the progressive fracture cannot be captured after the damage zone is fully developed because specimens fail catastrophically. To study the scaling of the post-initiation fracture response, in-plane scaled OCT specimens are tested in the present study.

Gonzales and Knauss [8] investigated the scaling of global fracture behaviour of large laminated composites by testing in-plane scaled compact tension specimens of two different stacking sequences and three different sizes. Structural scale compact tension specimens with notch lengths of 55.0 mm, 110.0 mm and 165.0 mm were tested. The results indicated that scaling can be related to the square root of the linear specimen or crack dimension. They also examined the damage at the ‘global crack front’ through 2-D X-ray images. Laffan et al. [9] studied the in-plane size effects in scaled cross-ply compact tension laminates. Compact tension specimens with scaled crack lengths of 26.0 mm, 32.0 mm and 37.0 mm were tested. They concluded that the R-curves for the three sizes are similar [10], which implies the scaling follows LEFM.

In the present paper, scaled quasi-isotropic OCT specimens are studied with notch lengths of 16.5 mm, 33.0 mm and 66.0 mm, covering coupon scale as well as structural scale laminates. Furthermore, more detailed damage development within each ply is examined through CT scanning. In particular, a fracture scenario is presented in which the damage development and fracture propagation are clearly distinguished. The applicability of the R-curve concept is also discussed.

2. Test setup

A schematic of the baseline OCT specimens is shown in Fig. 1. All baseline specimen dimensions are scaled down and scaled up by a factor of 2, so the in-plane scaled OCT specimens have notch lengths of 16.5 mm, 33.0 mm and 66.0 mm as shown in Table 1. The specimens were cut on a water jet cutting machine with finishing at the notch tip by a 1 mm-diameter cutter on a milling machine. The last three scaled up OCT specimens were manufactured with improved drilling quality for the holes, in order to achieve a better fit between the loading pins and the holes. An extensometer was attached to the loading pins to measure the Pin Opening Displacement (POD). The radii of the notch tips were r = 0.5 mm for all the OCT specimens. According to Camanho and Catalanotti [11] who used $[90/0/\pm45]_{3s}$ laminates and the same material in a compact tension test, the above notch radii are sharp enough for the results not to be affected by the notch tip radius.

The material used in this test was the Hexcel HexPly® IM7/8552 carbon-epoxy pre-preg with a nominal ply thickness of 0.125 mm. The lay-up for all the OCT specimens was $[45/90/\text{-}45/0]_{4s}$. The nominal overall thickness is 4 mm, which is very close to the actual thickness.

A steel test jig was developed to hold the OCT specimens in place, with arms to apply the vertical tensile load through loading pins. It was attached to an Instron hydraulic-driven test machine with a 100 kN load cell. The specimens were tested under displacement control with scaled loading rates with regards to the specimen dimensions (a loading rate of 1 mm/minute was used for the baseline specimens). A pair of anti-buckling bars was used in the baseline and the scaled-up OCT tests. They lightly clamped the rear end of those specimens to prevent potential buckling due to the high compressive stress caused by the in-plane bending of the specimens.

Interrupted tests, in which the tests were stopped after the first observed load drop, the first large load drop and a major load drop on the plateau of the load displacement curves were carried out as shown in Fig. 2. CT scanning was used to study the damage development in a single specimen from each interrupted test that was stopped at the different load levels. The samples from interrupted tests were soaked in a bath of zinc iodide penetrant for 3 days. A Nikon XTH225ST CT scanner was used to scan the scaled composite specimens from the interrupted tests. It has a 1 micron focal spot size and 225kV, 225W microfocus X-ray source.

3. Load-POD response

The fracture response in the baseline OCT test is divided into four stages on the typical load-POD curve in Fig. 2, which are linear loading, damage process zone development, fracture propagation, fracture zone expansion followed by final failure.

Load-POD curves of all the different sized OCT specimen tests are shown in Figs 3 to 5. At the beginning, the loads increase linearly with PODs. Then the first small load drops occur in the smaller two series of OCT tests, but this cannot be observed in the largest OCT tests. Thereafter, larger load drops are observed when the damage zone is fully developed, which is later demonstrated by CT images. After several major load drops, the specimens suffer final failure. The final failure events for the different sizes of OCT specimens were not identical. Specifically, the scaled down and the baseline OCT specimens suffered compressive failure at the rear end at the very end of the test. By contrast, the scaled up OCT specimens buckled after a short period of stable fracture growth after the peak loads.

Variation in the quality of fit of the loading pins in the holes in some scaled up OCT tests may affect the displacement measurements, and therefore affect the initial stiffness, as shown in Fig. 5. However, the failure initiation loads in the scaled up tests are highly consistent, with a C.V. of only 1.8%. These load values are later used for comparisons rather than the initial stiffness.

4. Damage development and fracture propagation

Interrupted tests and CT scanning for specimens of each size were carried out to study the failure mechanisms. CT images show the damage within typical plies with different fibre orientations in Figs 6 to 13. Damage in all the single 0 degree plies is similar, but significantly different in the double zero plies at the symmetry plane. Damage in all the ±45 degree plies is also similar except for the surface 45 degree plies, where no fibre breakage occurred during the tests. The amount of delamination observed is small during the damage process zone development, but quite substantial adjacent to the central double 0 degree plies in the later stages of fracture propagation. The surface 45 degree plies delaminate and split because they are unconstrained, which is why the fibres do not break.

4.1. Scaled down OCT tests

In the scaled down OCT specimens, splits initiate from the notch tips due to the high intra-laminar stress at the beginning of the damage zone development stage. At the first observed load drop, fibres break in the single 0 degree plies as shown in Fig. 6 b). Similar breakage also occurs in the other single zero plies. The splits in the central double 0 degree ply block are much longer than in the other 0 degree plies, blunting the stress concentration enough to prevent fibre breakage. All the ±45 degree plies are still intact at this very first observed load drop. During this period, the damage zone is developing. New splits form at the ends of the fibre fracture in the 0 degree plies.

At higher load levels, the central double 0 and ±45 degree plies begin to break which marks the end of the damage development, as shown in Fig. 7. When all the 0 degree and ±45 degree plies are broken, except for the surface 45 degree plies, the damage zone is fully developed and the fracture starts to propagate, i.e. the initial crack starts to extend.

As the fracture propagates, the split in the double 0 degree plies extends a long way and significant delamination occurs as shown in Fig. 8. This causes a sudden loss of stiffness in the specimens, and major load drops are observed on the load-POD curves. The damage zones are greatly enlarged due to such delamination, and extend across almost the whole region between the two loading pins. So the damage zones cannot be self-similar afterwards. In addition, the fracture is not within a narrow band ahead of the crack tip, so the specimen is effectively too small and the test data can no longer be used from this point on to determine fracture properties. Finally, the scaled down OCT specimens experience compressive failure at the rear end of the specimens, which marks the end of the tests.

4.2. Baseline OCT tests

In the baseline OCT specimens, fibre breakage occurs in all the 0 degree plies at the first observed load drop during the damage process zone development as shown in Fig. 9. However, ±45 degree plies are still not broken. The breakage of the ±45 degree plies marks the beginning of fracture propagation, when the damage zone in the baseline

OCT specimen is fully developed, as is shown in Fig. 10.

The baseline OCT specimens also show a fracture expansion stage with the rapid growth of delamination adjacent to the double 0 degree ply block at the symmetry plane of the specimen as shown in Fig. 11. The delamination area extends as far as the loading pin, which indicates that the specimen is not big enough to generate a relatively small-scale damage zone and the test data can no longer be used from this point onwards. At the final stage of the test, the baseline OCT specimens experience compressive failure at the rear end of the specimens.

4.3. Scaled up OCT tests

In the scaled up tests, the ±45 degree plies break at the first large load drop when the damage zone is already fully developed, as shown in Fig. 12.

Similar to the smaller-sized OCT specimens, the damage zone expands to a large extent due to splitting and delamination in the central double 0 degree ply block at a higher load level as shown in Fig. 13. The large damage zone implies that the specimen is still not big enough and the test data can no longer be used from this point. Finally, the scaled up OCT specimens buckle after the peak loads are reached. The loads stop increasing, and the tests are stopped.

4.4. Damage process zone comparison

Here, the damage zone is considered as the region ahead of the crack tips which consists of splitting, delamination, and some broken 0 degree and ±45 degree plies before the global crack front propagates (i.e. all the plies are broken, except for the surface plies). The distances between the last split and the crack tip in all of the 0 degree plies were measured from the CT images of the specimens from the interrupted tests in which the ±45 degree plies broke, except for the surface 45 degree plies. The average distance was used to determine the size of the fully developed damage zone. The sizes of the fully developed damage zones in the scaled down, baseline and scaled up OCT specimens from the interrupted tests are 2.6 mm (C.V. 17.6%), 2.8 mm (C.V. 25.7%), and 2.2 mm (C.V. 39.0%) respectively. The average size of the damage zone for all sizes is 2.5 mm.

5. Scaling of fracture response

If the scaling of fracture response of the in-plane scaled OCT specimens follows LEFM, the scaling of the fracture load should be proportional to the square root of the notch length. To verify if the fracture mechanics scaling prevails, a scaling correction according to reference [8] was carried out. In Fig. 14, the loads and PODs are scaled with respect to the baseline ones for a typical case of each of the three sizes of specimens. Loads and PODs are both multiplied by $2^{0.5}$ and $2^{-0.5}$ for the scaled down and scaled up specimens respectively (no scaling for the baseline specimen). Fig. 14 demonstrates that the three typical scaled load-POD curves collapse onto each other within the experimental scatter during the linear loading, damage process zone development and initial fracture propagation stages. This implies that the fracture toughness for initial propagation of fracture is independent of specimen sizes. Two of the curves also collapse onto each other beyond this stage until the major load drops, but the third curve from the scaled up tests, in which there is a larger variation in the load-POD curves, is slightly different. After the major load drops, the CT images show large amounts of delamination at the central double 0 degree ply block, the test data can no longer be used because of the large extent of damage.

The LEFM scaling also prevails when using the multiple specimen test data. In Fig. 15, loads from the multiple specimen tests at which the damage zones are fully developed are scaled for the three sizes of specimens with respect to the baseline ones. The selection of the load in the multiple specimen tests was according to the level at which the damage process zones are established, based on the carefully examined CT scanning after the interrupted tests. In the scaled down tests, the ±45 degree plies break at the first large load drop (7.02 kN, C.V. 4.3%) from tests of three specimens. For the baseline OCT tests, the ±45 degree plies break at the first large load drop (9.78 kN, C.V. 1.4%) from the tests of three specimens. For the scaled up tests, the ±45 degree plies are broken even at the first large load drop (14.49 kN, C.V. 1.8%) from tests of three specimens. As before, loads were multiplied by $2^{0.5}$ and $2^{-0.5}$ for the scaled down and scaled up OCT specimens respectively (no scaling for the baseline specimen). The results are similar within the experimental scatter, confirming that the scaling of the initial propagation of fracture is according to LEFM for $[45/90/-45/0]_{4s}$ OCT laminates.

6. Discussion

Gonzales and Knauss [8] studied three different sizes of two layups concluding that the ‘size-scaling’ they found was according to fracture mechanics. Laffan et al. [10]

used the same material to the one used in the present study but with a cross-ply stacking sequence. They concluded that there is no significant effect of scaling the specimen size with regards to fracture toughness. On the other hand scaled centre-notched tests of the same material and stacking sequence as used in the present paper showed that scaling is not in accordance with fracture mechanics for the small specimens. Only when the specimens with different notch sizes are big enough, are they asymptotic to the fracture mechanics scaling line [7]. The present study is consistent with the previous results for compact tension tests with stable crack propagation. The discrepancy with the centre-notched tests can be explained by the damage process zone development. In the in-plane scaled centre-notched tests, the size of the damage zone scales with specimen size for smaller specimens. The damage zone size increases gradually with specimen size towards a constant value for the large specimens. The average size (2.5 mm) of the damage zones in the scaled OCT is comparable to the measured value (2.3 mm) in large centre-notched specimen with a notch length of 25.4 mm and the same material and stacking sequence [7]. In the OCT tests the crack propagates stably, and so it is possible to capture the fully developed damage zone.

In another previous study [12], the stacking sequence effects in the baseline OCT tests have been investigated. It was found that the difference in the failure initiation loads in the dispersed-ply quasi-isotropic laminates $[45/90/-45/0]_{4s}$ (with a double central 0 degree ply block) and $[90/45/0/-45]_{4s}$ (without a double central 0 degree ply block) is not significant. Therefore, the fracture toughness for initial fracture propagation is not likely to be affected by the double central 0 degree ply block in the dispersed plies.

There are still some questions regarding a definitive fracture energy value from the OCT tests. Li et al. [6] applied the ASTM E399 standard to calculate the trans-laminar fracture energy in the baseline OCT tests of the same material and layup. The stress intensity factor expression in the ASTM E399 standard was originally calibrated for the standard compact tension configuration, rather than the OCT configuration. However, it can still be used for comparison purposes based on the actual results from the OCT tests. The key point is that the understanding and careful examination of the damage development and fracture propagation are crucial in terms of the selection of the appropriate failure loads, regardless of the absolute fracture energy value. In the OCT tests, the Mode I fracture toughness is proportional to the chosen failure load (P), so the Mode I fracture energy is proportional to the chosen failure load squared (P^2). Li et al. [6] chose the load level at the first significant load drop (P_{lam} = 9.36 kN, C.V. 2.7%), resulting in a fracture energy G_{IC_lam} = 61.4 kJ/m^2. In the present study, we carefully examined the damage at the notch tip at both the first observed load drop (P_i = 8.85 kN, C.V. 5.3%), and the first large load drop (P_0 = 9.78 kN, C.V. 1.4%) corresponding to all plies breaking except for the surface plies. According to the ASTM E399 standard, the calculated fracture energy G_{0_ASTM} = 67.1 kJ/m^2 using P_0 is only slightly higher than G_{IC_lam} of the same material and layup determined previously considering the scatter. By contrast, the calculated 'fracture energy' G_{i_ASTM} = 54.9

kJ/m^2 using P_i is much lower. All calculated fracture energy values, the loads used and the damage zone sizes are presented in Table 2. As presented in the CT images of the baseline specimen, at the first observed drop, the damage process zone is not fully developed, so the 'fracture energy' calculated using P_i is not the true value for fracture propagation or an intrinsic property of the material. In general, different fracture energy values can be calculated by choosing either the load level at the first observed load drop or the peak load level for the OCT tests. Such calculated 'fracture energy' values may not represent the true fracture property of the material because at the first observed load drop the damage zone may not be fully developed, whilst later in the test the damage zone may be too large compared with the specimen size.

An R-curve describes the relation between the resistance to fracture and the propagation of crack length. Often, such resistance to fracture increases as the crack grows. In the present study, it is found that during the damage process zone development stage, the applied load increases and fracture resistance apparently increases for the small specimens. However, the initial crack does not extend because the ±45 degree plies are still intact, so this period should not be interpreted as an R-curve, but as the development of the damage zone. During the late fracture propagation stage, the applied load increases, reaching a peak value and fracture resistance apparently increases again. However, the damage zone at the double 0 degree ply block expands outside the loading pins due to substantial splitting and delamination. The experimental data can no longer be used in this region and therefore do not necessarily indicate an R-curve either. This shows the need for caution when determining R-curves for composite materials considering their complex nature during damage development and fracture propagation.

7. Conclusions

The fracture toughness for initial propagation of fracture of in-plane scaled OCT quasi-isotropic IM7/8552 laminates is independent of specimen size on condition that the damage zone is fully developed. The sizes of the fully developed damage zones for OCT specimens of different sizes are similar, and they are also comparable to the measured damage zone size from large centre-notched tests of the same material and stacking sequence.

The sizes of even the largest $[45/90/-45/0]_{4s}$ OCT specimens used in this study are too small to generate self-similar crack growth with a small scale damage zone throughout the tests for this material and layup. During the tests of all sizes of specimens, the delamination grows rapidly at the central double 0 degree plies at high load levels, connecting the multiple 0 degree splits. As a result, the damage zone expands to such a large extent that it sometimes goes beyond the region between the loading pins. Consequently, the present OCT tests can only capture a short period of progressive fracture during the initial propagation stage, after which the test data can no longer be used. Nevertheless, this is enough to generate a fully developed damage zone.

The present study highlights the need for caution in applying the R-curve concept to composite materials. The apparent increase of fracture resistance with crack length may be either due to the development of the damage zone before all the plies are broken throughout the specimen thickness, or because the damage zone has become too large in comparison with the specimen size, for example because of the large amount of splitting and delamination in the central double 0 degree ply block in the current study.

References

[1] ASTM, Standard, E399-90. Standard test method for plane-strain fracture toughness of metallic materials. West Conshohocken, PA, USA: ASTM International; 1990 (1997).

[2] ASTM, Standard, E1922-97. Standard test method for translaminar fracture toughness of laminated polymer matrix composite materials. West Conshohocken, PA, USA: ASTM International; 1997.

[3] Kongshavn I, Poursartip A. Experimental investigation of a strain-softening approach to predicting failure in notched fibre-reinforced composite laminates. Composites Science and Technology. 1999;59(1):29-40.

[4] Floyd AM. An engineering approach to the simulation of gross damage development in composites laminates. Vancouver, Canada: PhD Thesis, The University of British Columbia; 2004.

[5] Williams KV, Vaziri R, Poursartip A. A physically based continuum damage mechanics model for thin laminated composite structures. International Journal of Solids and Structures. 2003;40(9):2267-300.

[6] Li X, Hallett SR, Wisnom MR, Zobeiry N, Vaziri R, Poursartip A. Experimental study of damage propagation in Over-height Compact Tension tests. Composites Part A: Applied Science and Manufacturing. 2009;40(12):1891-9.

[7] Xu X, Wisnom MR, Mahadik Y, Hallett SR. An experimental investigation into size effects in quasi-isotropic carbon/epoxy laminates with sharp and blunt notches. Composites Science and Technology. 2014;100(0):220-7.

[8] Gonzáles L, Knauss WG. Scaling global fracture behavior of structures-sized laminated composites. International Journal of Fracture. 2002;118(4):363-94.

[9] Laffan MJ, Pinho ST, Robinson P, Iannucci L. Measurement of the in situ ply fracture toughness associated with mode I fibre tensile failure in FRP. Part I: Data reduction. Composites Science and Technology. 2010;70(4):606-13.

[10] Laffan MJ, Pinho ST, Robinson P, Iannucci L. Measurement of the in situ ply fracture toughness associated with mode I fibre tensile failure in FRP. Part II: Size and lay-up effects. Composites Science and Technology. 2010;70(4):614-21.

[11] Camanho PP, Catalanotti G. On the relation between the mode I fracture toughness of a composite laminate and that of a 0° ply: Analytical model and experimental validation. Engineering Fracture Mechanics. 2011;78(13):2535-46.

[12] Xu X, Wisnom MR, Hallett SR, Zobeiry N, Leslie S, Poursartip A, Vaziri R. Stacking sequence effects in over-height compact tension tests of quasi-isotropic laminates. 19th International Conference on Composite Materials. Montreal, 2013.

List of captions of figures:

1. Schematic of the baseline OCT specimen.

2. Typical load-POD curve from the baseline OCT test. a) Linear loading; b) Damage process zone development; c) Fracture propagation; d) Fracture zone expansion

3. Load-POD curves from the scaled down OCT tests.

4. Load-POD curves from the baseline OCT tests.

5. Load-POD curves from the scaled up OCT tests.

6. CT images of the scaled down OCT specimen at 6.1 kN (first observed load drop).

7. CT images of the scaled down OCT specimen at 6.9 kN (first large load drop).

8. CT images of the scaled down OCT specimen at 7.5 kN (major load drop).

9. CT images of the baseline OCT specimen at 8.9 kN (first observed load drop).

10. CT images of the baseline OCT specimen at 9.9 kN (first large load drop).

11. CT images of the baseline OCT specimen at 11.2 kN (major load drop).

12. CT images of the scaled up OCT specimen at 14.2 kN (first large load drop).

13. CT images of the scaled up OCT specimen at 18.5 kN (major load drop).

14. Scaling correction of the typical load-POD curves for scaled OCT specimens. Loads and PODs are multiplied by $2^{0.5}$ and $2^{-0.5}$ for the scaled down and scaled up OCT specimens respectively (no scaling for the baseline specimen).

15. Scaled failure loads in scaled multiple specimen OCT tests. Loads are multiplied by $2^{0.5}$ and $2^{-0.5}$ for the scaled down and scaled up OCT specimens respectively (no scaling for the baseline specimen).

List of captions of tables:

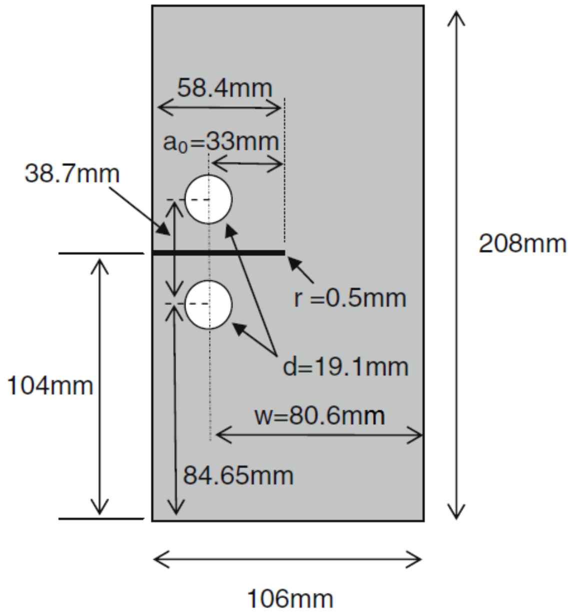
58.4mm
a_0=33mm
38.7mm
208mm
r =0.5mm
d=19.1mm
104mm
w=80.6mm
84.65mm
106mm

Fig. 1

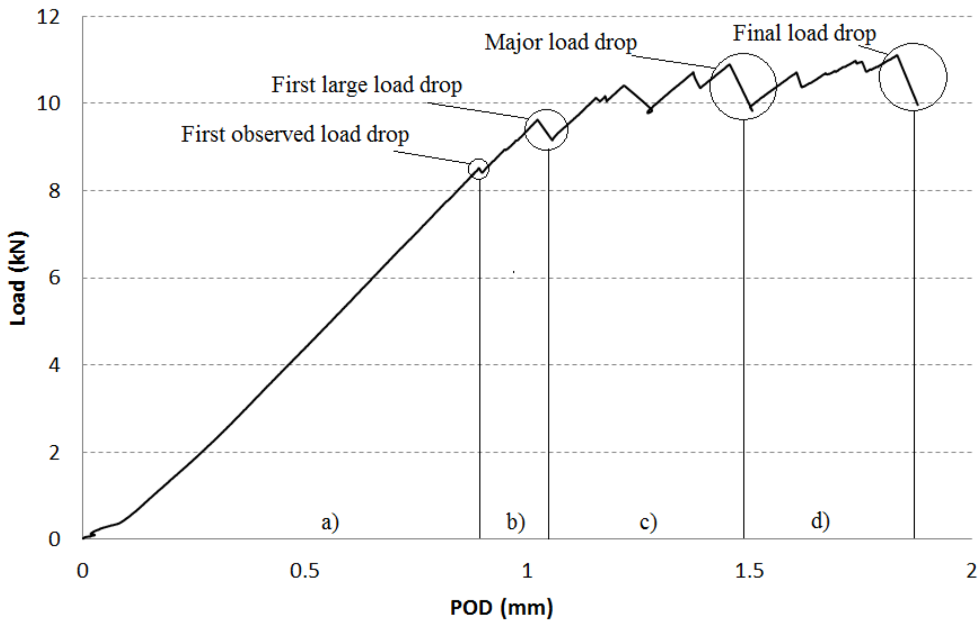
Major load drop
Final load drop
First large load drop
First observed load drop
Load (kN)
POD (mm)
a)
b)
c)
d)
0
2
4
6
8
10
12
0
0.5
1
1.5
2

Fig. 2

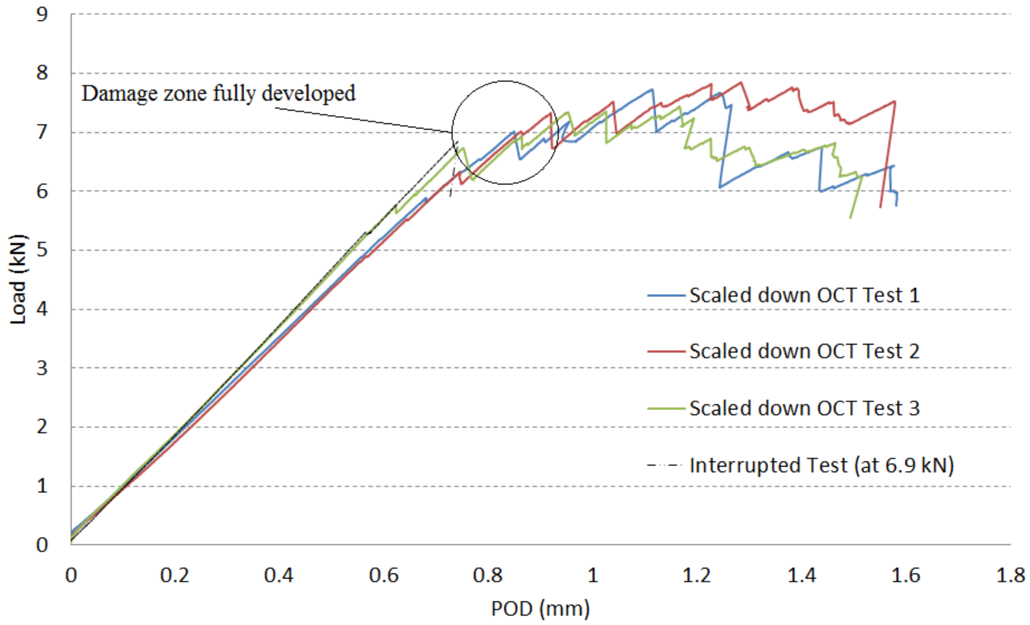

Damage zone fully developed
Load (kN)
POD (mm)
Scaled down OCT Test 1
Scaled down OCT Test 2
Scaled down OCT Test 3
Interrupted Test (at 6.9 kN)

Fig. 3

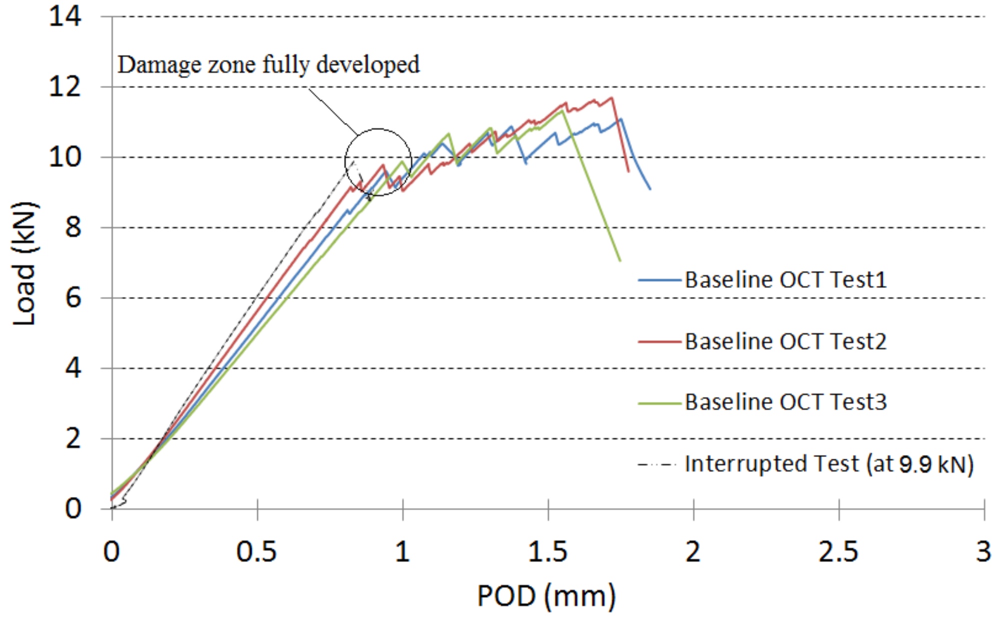

Damage zone fully developed
Load (kN)
POD (mm)
Baseline OCT Test1
Baseline OCT Test2
Baseline OCT Test3
Interrupted Test (at 9.9 kN)

Fig. 4

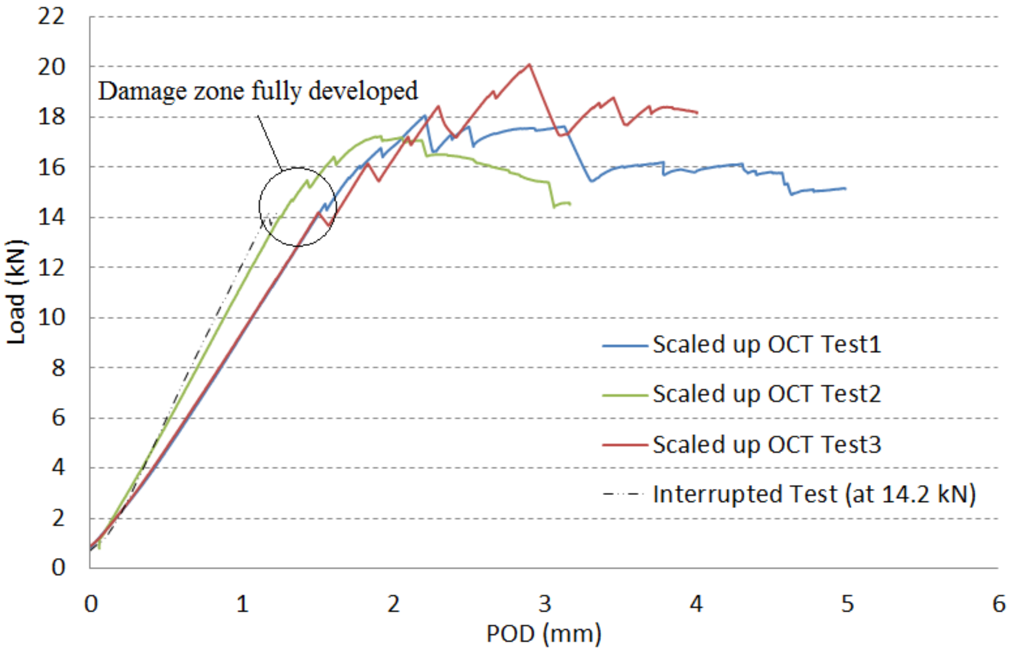

Damage zone fully developed
Load (kN)
POD (mm)
Scaled up OCT Test1
Scaled up OCT Test2
Scaled up OCT Test3
Interrupted Test (at 14.2 kN)
0
2
4
6
8
10
12
14
16
18
20
22
0
1
2
3
4
5
6

Fig. 5

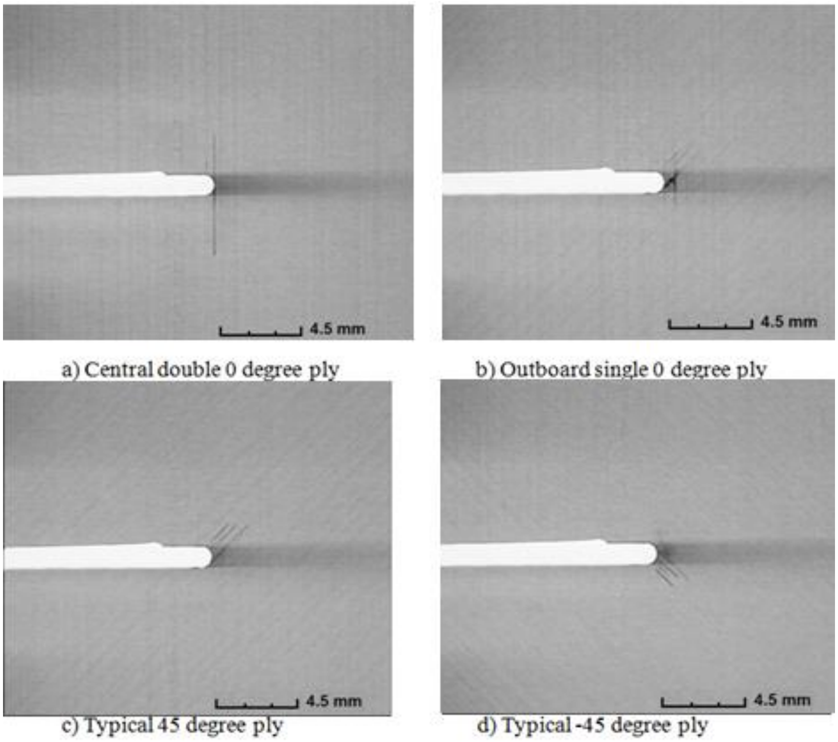

4.5 mm
a) Central double 0 degree ply
4.5 mm
b) Outboard single 0 degree ply
4.5 mm
c) Typical 45 degree ply
4.5 mm
d) Typical -45 degree ply

Fig. 6

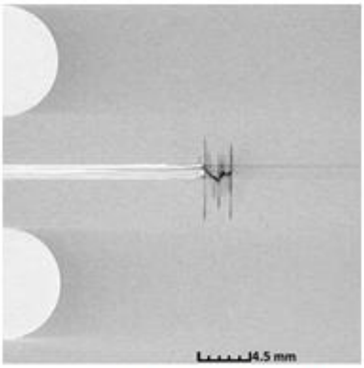

a) Central double 0 degree ply

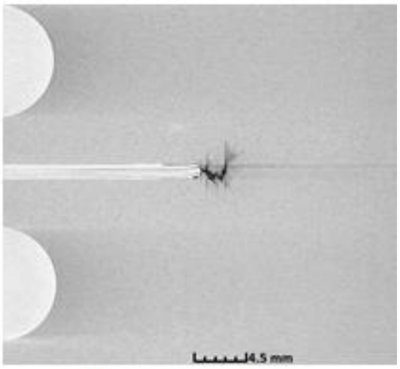

b) Outboard single 0 degree ply

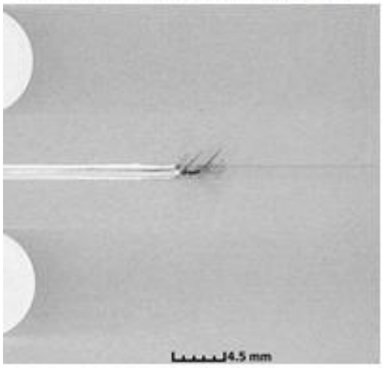

c) Typical 45 degree ply

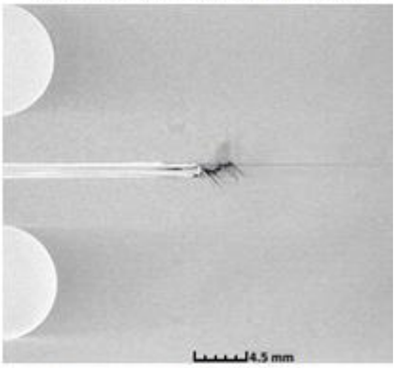

d) Typical -45 degree ply

Fig. 7

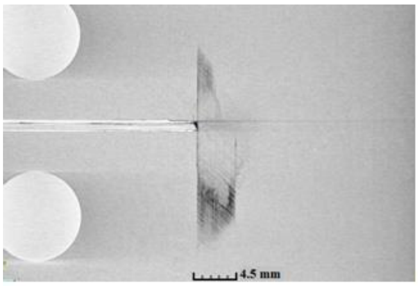

a) Central double 0 degree ply

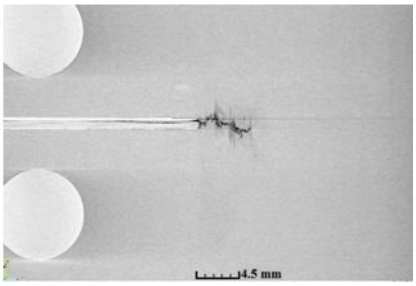

b) Outboard single 0 degree ply

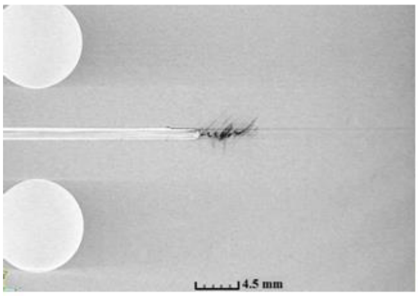

c) Typical 45 degree ply

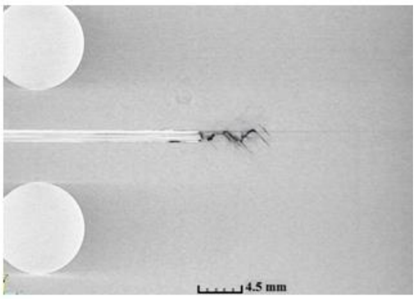

d) Typical -45 degree ply

Fig. 8

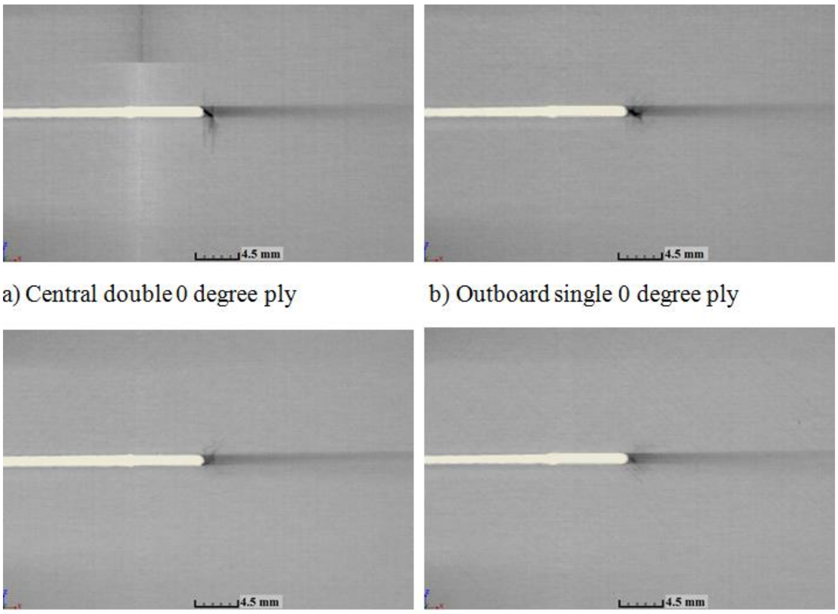

a) Central double 0 degree ply

b) Outboard single 0 degree ply

c) Typical 45 degree ply

d) Typical -45 degree ply

Fig. 9

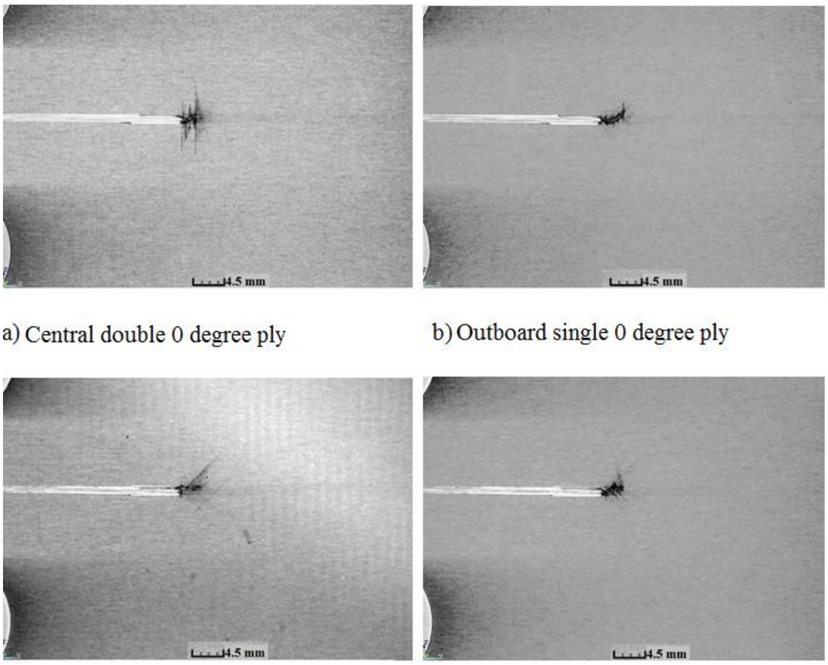

a) Central double 0 degree ply

b) Outboard single 0 degree ply

c) Typical 45 degree ply

d) Typical -45 degree ply

Fig. 10

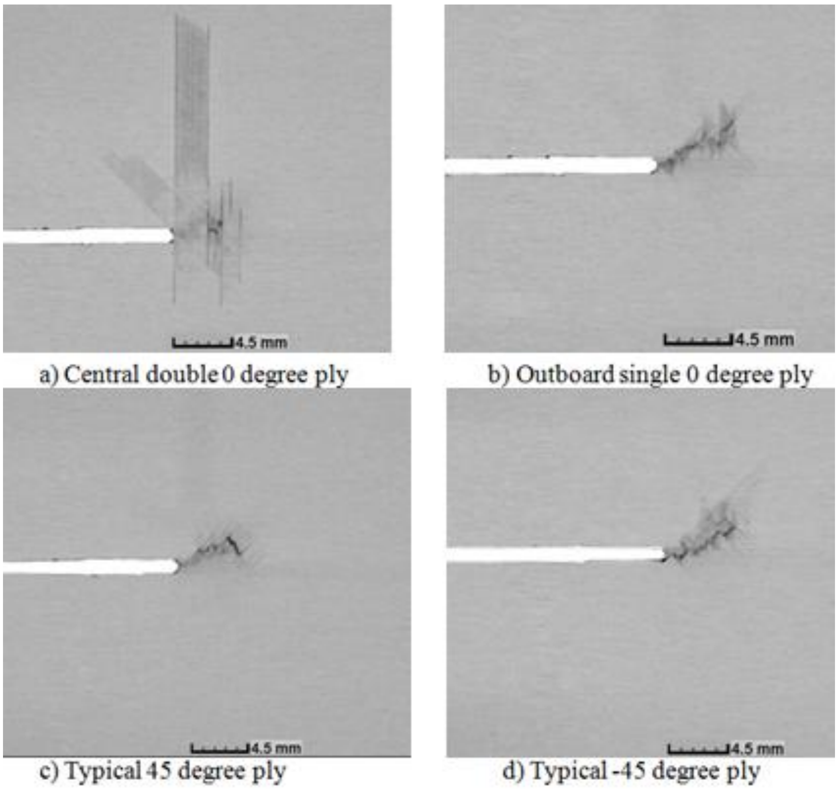

a) Central double 0 degree ply
b) Outboard single 0 degree ply
c) Typical 45 degree ply
d) Typical -45 degree ply

Fig. 11

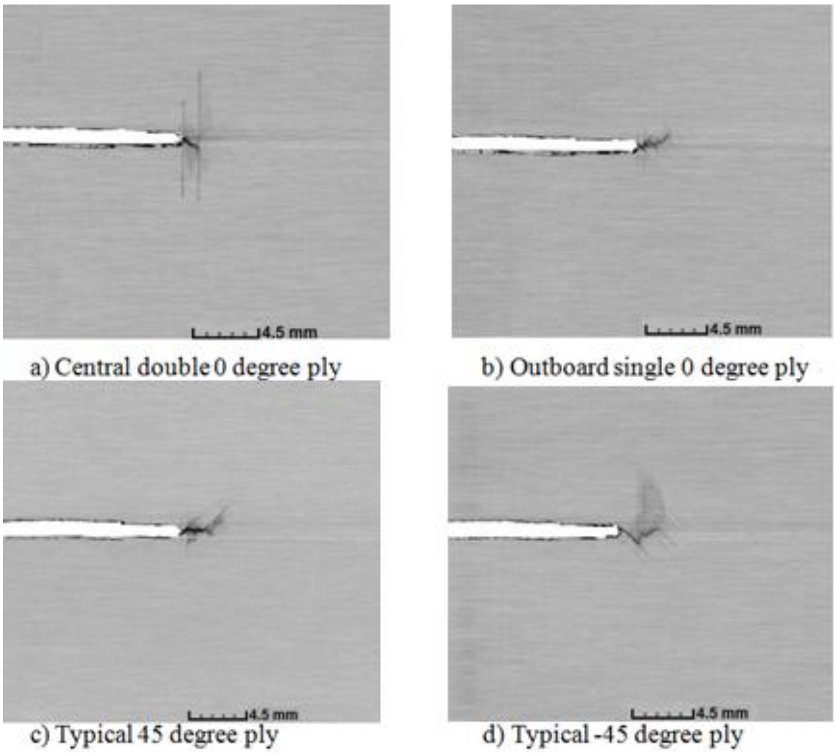

a) Central double 0 degree ply
b) Outboard single 0 degree ply
c) Typical 45 degree ply
d) Typical -45 degree ply

Fig. 12

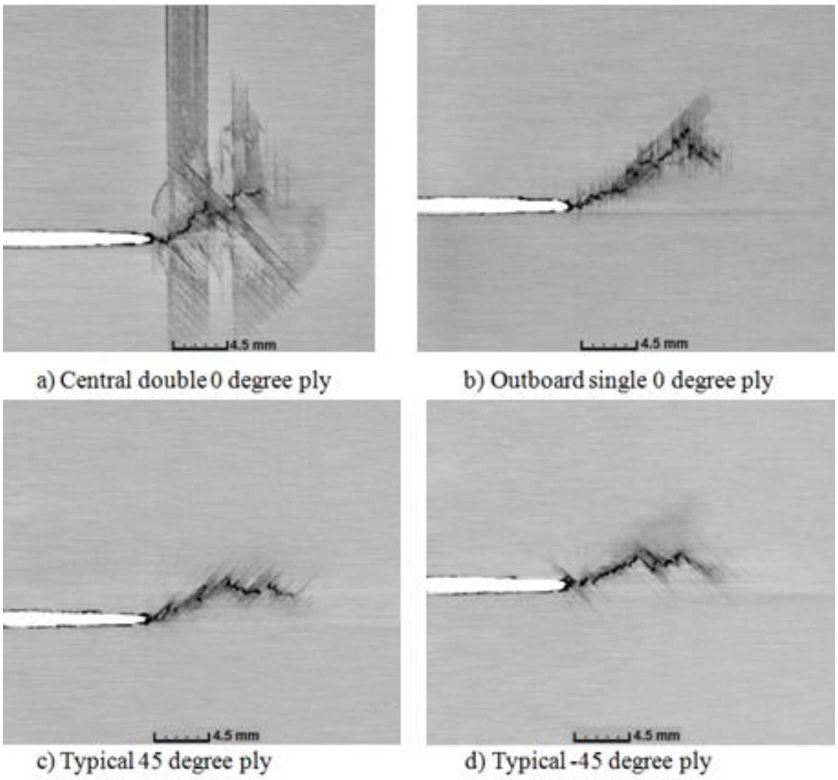
4.5 mm
a) Central double 0 degree ply
4.5 mm
b) Outboard single 0 degree ply
4.5 mm
c) Typical 45 degree ply
4.5 mm
d) Typical -45 degree ply

Fig. 13

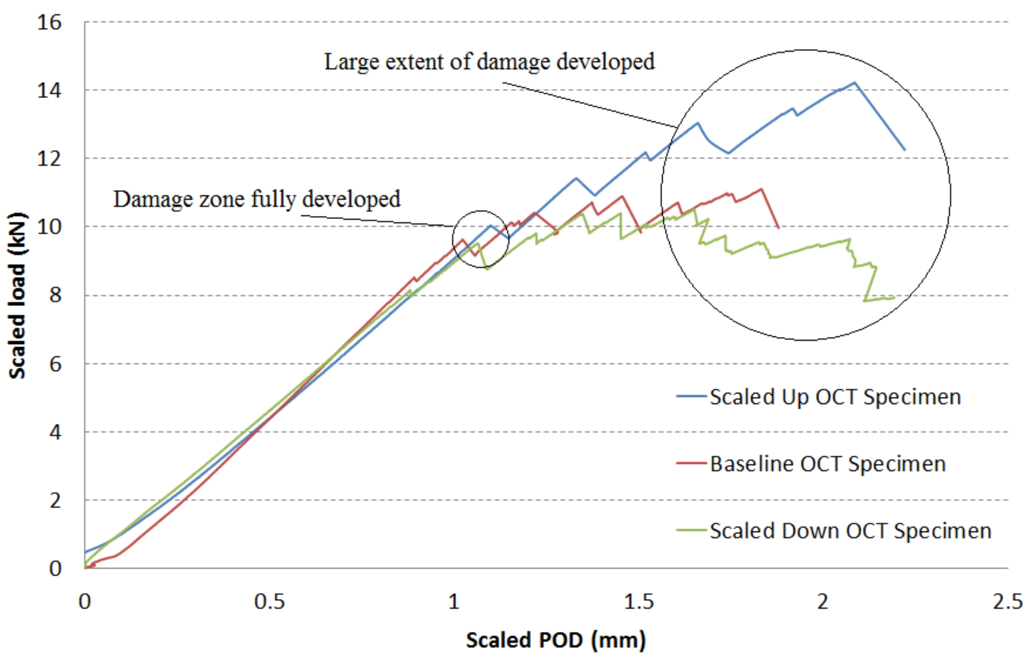
Large extent of damage developed
Damage zone fully developed
Scaled load (kN)
Scaled POD (mm)
Scaled Up OCT Specimen
Baseline OCT Specimen
Scaled Down OCT Specimen
0
2
4
6
8
10
12
14
16
0
0.5
1
1.5
2
2.5

Fig. 14

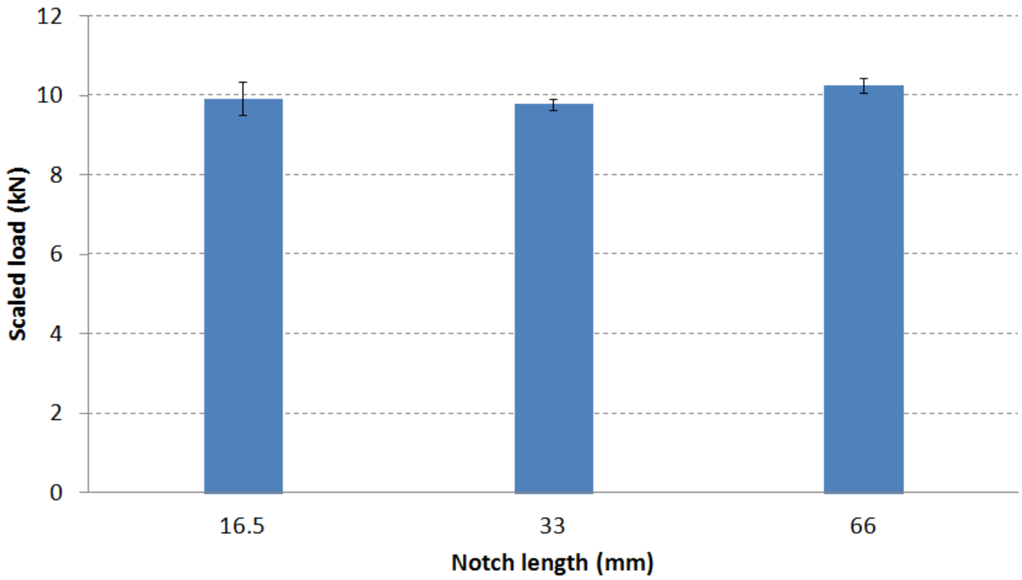

Fig. 15

Table 1

Specimen	Width	Height	Notch length	Notch radius	Hole diameter
Scaled down	53.0	104.0	16.5	0.5	9.6
Baseline	106.0	208.0	33.0	0.5	19.1
Scaled up	212.0	416.0	66.0	0.5	38.2

Table 2

Specimen	Failure load (kN) (C.V. %)	Fracture energy (kJ/m^2) (C.V. %)	Damage zone size (mm) (C.V. %)
Scaled down	7.02 (4.3%)	69.1 (8.7%)	2.6 (17.6%)
Baseline	9.78 (1.4%)	67.1 (2.8%)	2.8 (25.7%)
Scaled up	14.49 (1.8%)	73.6 (3.7%)	2.2 (39.0%)